FEATURE ARTICLE

Diffusive Relaxations and Vibrational Properties of Water and H-bonded Systems in Confined State by Neutrons and Light Scattering: State of the Art

Vincenza Crupi, Domenico Majolino, Placido Migliardo,* and Valentina Venuti

Department of Physics, Messina University and INFM Section of Messina, C.da Papardo, S.ta Sperone 31, P.O. Box 55, 98166 S. Agata, Messina, Italy

Received: May 10, 2000; In Final Form: August 1, 2000

A detailed spectroscopic analysis is presented in order to study the reorientational and vibrational dynamics of water and other fundamental H-bonded systems: ethylene glycol ($HO-CH_2-CH_2-OH$) and its homologous species, such as ethylene glycol monomethyl ether ($CH_3O-CH_2-CH_2-OH$) and ethylene glycol dimethyl ether ($CH_3O-CH_2-CH_2-OCH_3$), propylene glycol ($HO-CH(CH_3)-CH_2-OH$) and its oligomers, that are confined in a matrix of sol−gel porous glasses with 26 Å interconnected cylindrical pores. The use of different spectroscopic techniques, light scattering (Rayleigh wing and Raman scattering), FT-IR absorption, neutron scattering (incoherent quasi elastic and inelastic neutron scattering, IQENS and IINS, respectively) allow the marking of different dynamical parameters, with different probes being used to investigate H-bonded systems. The clear influence of the confinement on the mobility of the studied liquids, with a dramatic frozen-in observed effect respect to the bulk state, is evidenced and compared with literature results. Furthermore, a surface−liquid potential well induces strong modifications of the local symmetry of the vibrational groups (e.g., the active OH stretching groups) involved in the interaction, giving rise to anharmonic effects (red shift, band enlargement) that depend on the nature of the surface (hydrophobic or hydrophilic) and on the nature of guest liquids (wetting or nonwetting).

I. General Considerations

The investigation of the structural and dynamical properties of liquids confined in various host matrices has been studied for a long time, and is still a subject of current interest.[1−4] For a complete and very recent summary in the confinement field, the reader can refer to the report of International Workshop on Dynamics in Confinement, Proceedings (Grenoble, France, January 26−29, 2000); *J. Phys. IV* **2000,** *10* and references therein. Experimental techniques and theoretical approaches have shown that the physical properties are modified relative to the bulk values when the size of the confining pores is in a few nanometer range. This topic is also of technological significance in the chemical−physical world, for example, for chromatographic separation of polymers, enhanced oil recovery, membrane separation, lubrication, and polymerization in the presence of heterogeneous catalysts.[5] Several studies have been devoted to the confinement effects of different fluids, ranging from small inorganic molecules (water), organic aliphatic materials (simple glass-forming materials) to complex systems such as polymers, mainly in nanoporous materials.[6] Structures suitable for the study of hindered transport in restricted geometries are, for example, zeolites, silica gels and aerosil, aluminum oxides, hydroxides or alumino-silicates, and porous polymer membranes. Also reversed micelles can be considered as useful confinement method, and they have received particular attention in recent years. Thermodynamic and spectroscopic properties of liquids in reversed micelles have been studied by means of many experimental techniques.[7−9] In particular, Santucci et al.[7] analyzed the structure of water in bis(2-ethylhexyl) sodium sulfosuccinate (AOT) micelles as a function of the $[H_2O]/[AOT]$ ratio (W) by using the IR absorption due to the O−H stretching modes in the 3800−3000cm^{-1} and the1928 nm absorption of water usually assigned to a combination mode of asymmetric stretching and bending vibrations. The results showed that the IR spectra could be expressed as sum of contributions from interfacial and bulklike water. The fraction of water in the two "regions" within the water pool was evaluated as a function of W. On increasing W, the IR spectra change significantly up to $W \sim 6$ and then, at higher water contents, gradually approach those of bulk water.

In general, the role of a surface in modifying the behavior of bulk liquid is difficult to study experimentally, since the region of interest consists of a layer whose thickness is usually quite small. For increasing the surface-related effect relative to that from the bulk liquid, *porous silica glasses* were chosen as optically transparent substrate materials. In particular their large pore surface area, highly interconnected pores, narrow pore size distribution, chemical and mechanical stability, transparency and huge inner surface, can be chemically modified to reduce the surface polarity, making these glasses an ideal host medium in studies of molecular dynamics in confined geometries. These kinds of glasses are prepared with controlled average pore sizes

* Corresponding author. Department of Physics, Messina University and INFM Section of Messina, C.da Papardo, S.ta Sperone 31, P.O. Box 55, 98166 S. Agata, Messina, Italy. Tel: +39090391478. Fax: +39090395004. E-mail: migliard@dsme01.messina.infm.it.

10.1021/jp001736l CCC: $19.00
Published on Web 10/19/2000

from a few angstroms to a few tens of a micrometer, with a sol−gel technique that yields an homogeneous material basically free of contaminants.[10]

It has been generally observed that the diffusion of polymers in porous systems is slowed compared to the bulk state with increasing geometrical confinement. This was interpreted by geometric as well as by adsorption effect.[11] They are respectively related to the extent to which pores are dead ended and tortuous (geometry, physical effects) and to the degree the diffusing molecules are adsorbed on the surface sites (chemistry, chemical effects).[12] The separation of the contributions of *physical* and *chemical traps* is still a noncompletely solved problem. Generally speaking a lot of studies demonstrated the existence of two well separated dynamical processes: the first one is associated with the dynamics of the bulklike molecules, largely unaffected by the pores, and is governed by intermolecular interactions (i.e., van der Waals or hydrogen bonding forces), by the shape of the molecules, collective hydrodynamic effects, etc. The second one is connected to an interfacial layer of molecules strongly influenced in their reorientational dynamics, which leads to partial local order induced by the dipole−dipole interactions as well as to the slowing down of dynamic processes. The dynamics of these adsorbate molecules, directly attached to the pore walls, is substantially triggered by surface forces which can be attractive or repulsive, depending on the polarity, adsorption energies, and surface coverage. For our investigated systems the inner surface of the pores possess active sites (silanol groups, SiOH) responsible of the specific interaction (Hydrogen-bond, HB) with the hydroxyl groups of the confined molecules, giving rise to structural and dynamical properties strongly modified respect to the bulk ones.

Examples of confinement effect include anomalous and lamellar diffusion, enhancement of correlation times, shift of melting and freezing temperatures, as well as the change of the very character of phase transition occurring in a space having dimension less than three (fractal path).[13,14] In particular geometrical restrictions are found to favor an increased microviscosity that causes a more hindered diffusion in the imbibed liquids and a molecular reorientation time longer than in the bulk state. The excluded volume effects[15] (i.e., physical traps) on the radial distribution functions have a physical origin that can be explained taking into account that the local number density n_l for an atom in the liquid phase in a pore is generally higher than the average number density of the liquid in the whole system $\bar{n}$, because the regions of the sample occupied by the substrate are forbidden for the atoms (frustration). It is a topologically effect, nonstrongly dependent on the details of the atomic interactions (hydrophilic or hydrophobic), the shape of the pores and the relative volume of the sample being the two factors that play the main role.

As far as the modified structural properties of a system near interfaces are concerned, some years ago J. C. Dore et al.,[16] carried out neutron diffraction studies for heavy water in two high surface area silica samples, Spherisorb (90 Å) and Gasil (20 Å). Their results showed that the structural molecular arrangement is very similar to that of bulk liquid and that the modification due to the substrate is restricted to a region within 10 Å or less of the interface. No evidence has been found that suggests that the nature of the liquid is substantially altered by interfacial interactions: at the most, dispersed water undergoes, in fact, significant structural changes with temperature variations, but the observed behavior is analogous to that of bulk liquid. This occurrence can be justified thinking that the geometric arrangement of atoms can occur in such a way that the water−surface H-bond does not alter the time averaged water structure.

Recently, P. Gallo et al.[17] reported molecular dynamics simulations (MD) of water confined in a cylindrical silica Vycor pore (40 Å), hydrophilic in nature. They put into evidence the dependence of microscopical structural and dynamical properties on the degree of hydration (from 19% to 96%) of the pore. It turns out that low amounts of water are almost completely adsorbed on the substrate surface, although some water molecules (hydrogen bonded to adsorbed molecules) are found in the second layer. The observed MD results showed a strong reduction of the water−water hydrogen bonds close to the pore surface, balanced by the increasing of the hydrogen bonds between water molecules and functional groups of the Vycor. With decreasing degree of hydration an increasing volume in the center of the pore is devoid of water molecules. When the highest hydration percentage is reached, the center appears as a continuous and homogeneous region, characterized by a density value lower than the bulk state. In addition, the self-diffusion coefficients of molecules in the inner pore volume appear to be higher if compared to the ones of interfacial molecules. The evaluated spectral densities of the center of mass of hydrogen atom motion are similar to those of the bulk near the center of the pore, while, close to the surface, the effects of confinement suffered by the molecules attached to the substrate are reflected and a strong modification of the "lattice" bands centered at $\sim$50 cm^{-1} and $\sim$200 cm^{-1}, due to intermolecular tetrahedral symmetry, is observed. Successively P. Gallo et al. found,[17] at the lowest hydration level, evidence of a "cage" effect with a flattening of the mean square displacement of the center of mass of water molecules similar to that observed in MD of supercooled bulk water. Furthermore, the authors show the formation of a double layer structure of water molecules close to the substrate, in which the molecules of the layer nearest to the surface are deeply frozen and show very slow relaxation. At the same time, the water molecules in the second layer relax with a nonexponential long time tail, well fitted by a Kohlrausch−Williams−Watt function, recalling effects rationalized in the mode coupling theory.

The investigation of the dynamical properties of liquids confined in sol−gel glasses has been carried out by a variety of techniques: between them, dielectric spectroscopy,[6] nuclear magnetic resonance (NMR),[18,19] optical Kerr effect (OKE),[20] Raman spectroscopy,[21,22] dynamic light scattering,[3,23−25] and neutron scattering[26,27] have proved particularly successful. The interpretation of the experimental spectra has been performed, by many authors, in terms of a two-state models[6] with dynamic exchange between a bulklike phase in the pore volume and an interfacial phase near the pore wall. In this way it has been possible to analyze in detail the interplay between the molecular dynamics in the two subsystems (bulklike and interfacial), its dynamic exchange, and hence their growth and decline in dependence on temperature and strength of the molecular interactions. Sometimes, a three-layer model is deduced,[28] consisting of molecules having solidlike, interfacial, and bulklike dynamics, respectively. In the first layer bulk properties are seriously distorted or eliminated, in the second one they are strongly modified because of the interaction with the surface, that can be attractive or repulsive, depending on the polarity. Finally, in the layer corresponding to the inner volume, close to the center of the pore, bulk properties are restored. It has been shown that while the bulklike fraction scales with the pore size, the interfacial and solidlike layers remaining relatively unchanged. In particular, as an example, J. T. Forkas et al.,[20]

performed a detailed investigation of nanoconfined weakly and strongly wetting liquids by OKE spectroscopy. This technique, that furnishes, as Rayleigh wing spectroscopy, the collective orientational correlation function on time scale ranging from femtoseconds to hundreds of picoseconds, is complementary to those spectroscopies, such as NMR and Raman, which measure single-molecule dynamics. The authors showed that in the case of weakly wetting liquids, the reorientational decay is described by the sum of two exponential and interpreted in terms of the above-described two states model, the first one characterized by the same time constant of bulk liquid and the other one having a significantly larger time constant. For strongly wetting liquids a triexponential decay is revealed, explained in terms of the three distinct populations (bulklike, interfacial and solidlike molecules) which contribute to the mentioned three states model.

To put in evidence dynamical spectroscopic response in a wide class of liquids, H-bonded and not, confined into 25 Å small pores of sol−gel silica glasses, having active sites for interaction or not, we present here a lot of experimental data, performed over the past few years by our research group, comparing them with theoretical models to elucidate the surface role on the liquid state properties. The aim was to investigate and clarify the effects, on the vibrational and reorientational dynamics of H-bonded (propylene glycol, PG, and its oligomers polypropylene glycols, PPG, with MW 425, 725, and 4000 Da; ethylene glycol, EG, and its homologous system, EG monomethyl ether, EGmE, and water) and non H-bonded (EG dimethyl ether, EGdE) liquids, of hydrophilic (Si−OH active groups present on the inner pore surface) and hydrophobic surfaces (Si−OCH_3 nonactive groups), obtained from the former by treatment.

Generally speaking, we focused our analysis on the following cases: (i) strongly interacting liquids near interacting surface (hydrophilic−hydrophilic interaction), (ii) strongly interacting liquids near non interacting surface (hydrophilic−hydrophobic interaction), (iii) noninteracting liquids near interacting surface (hydrophobic−hydrophilic interaction), and (iv) noninteracting liquids near noninteracting surface (hydrophobic−hydrophobic interaction).

Our research has been performed with the employment of different spectroscopies: light scattering (Rayleigh wing, Raman), Fourier transform infrared absorption, and neutron scattering. As it is well-known,[29] an useful way to mark the presence of various intermolecular conformations, H-bond imposed, is the investigation, by IR and Raman spectroscopies, in some detail of the vibrational properties of the active sites for the interactions, i.e., the O−H stretching region. In this spectral range (3000−3800 cm^{-1}) the presence of various subbands, shifted with respect to the fundamental OH mode (∼3630 cm^{-1}), gives rise to a broad spectral distribution, unambiguously indicating the appearance of different structural environments. On these bases, IR and Raman results have been proved to be very useful and complementary to better understand the spectral features of the complex Rayleigh wing spectra passing from the bulk to the confined samples.

Rayleigh wing data showed, for the analyzed H-bonded samples, an Havriliak−Negami profile[30] for the reorientational relaxation, indicating a distribution of relaxation time. For the non H-bonded system, EGdE, we will show that a Lorentzian profile is recovered because, in this case, the formation of any kind of intermolecular arrangement is impossible. This kind of analysis has been also applied for explaining incoherent quasi-elastic neutron scattering (IQENS) spectra of water, in bulk and confined into active surfaces, at different temperatures. It is well-known,[31] in fact, that, when hydrogenous molecules are examined, comparing the incoherent quasi-elastic neutron scattering (IQENS) rotational contributions with the Rayleigh wing ones could be a fruitful method in order to obtain relevant information about the existence of cooperative effects in the system under investigation. This happens because of the incoherent nature of the proton cross sections and because the neutron scattering technique probes the single-molecule diffusional motion more directly, giving information on the self-rotational relaxation time τ_s, whereas Rayleigh wing probes more directly the collective rotational relaxation time τ_c.

Another fundamental quantity, due to noncentral motions, obtained from our low- and very-low-frequency analysis performed by means of Raman, on one hand, and IINS experiments, on the other, is the generalized frequency distribution function $g(\omega)$.[32] It is well-known that this quantity is obtained by following the Egelstaff extrapolation procedure as

$$g^N(\beta) = 2\beta \sinh(\beta/2)(\lim_{\alpha\to 0} S_{inc}(\alpha, \beta)/\alpha)$$

where $\alpha = \hbar^2\mathbf{q}^2/2Mk_BT$, $\beta = \hbar\omega/k_BT$, with $\hbar$ being Planck's constant over 2π and $\mathbf{q}$ the wave vector. On the other hand, the depolarized Raman intensity I_{VH} furnishes the effective vibrational density of states $g^R_{eff}(\omega)$ connected to $g^N(\omega)$ through the relation $g^R_{eff}(\omega) = C(\omega)g(\omega) \equiv C(\omega)g^N(\omega)$, where $C(\omega)$ is the usual electron-vibration coupling factor, and $g^N(\omega)$ can be obtained, for example, from an IINS experiment. As it is shown in the sequel, both the $g^N(\omega)$ and $g^R_{eff}(\omega)$ show clear evidence, for example in the case of water, of surface-induced vibrational modes due to the local order distortion respect to the bulk one.

The remainder of the article has been schematized in the following way: in the next section we will describe the employed experimental methods. In section III we will discuss the reorientational and vibrational dynamics of relatively simple (water) and complex (EG and its homologous, PG and its oligomers) confined liquids, and our concluding remarks will be reported in section IV.

II. Experimental Methods

A. Nanoporous Glasses and Samples Preparation. IR absorption, Raman, Rayleigh wing, IQENS, and IINS measurements were performed on water, propylene glycol [PG: H(O−$CH(CH_3)$−CH_2)OH], polypropylene glycols [PPG: H(O−CH−(CH_3)−$CH_2)_n$OH], MW 425, 725, and 4000 Da, ethylene glycol [EG: H(O−CH_2−CH_2)OH], EG monomethyl ether [EGmE: CH_3(O−CH_2−CH_2)OH], and EG dimethyl ether [EGdE: CH_3(O−CH_2−CH_2)OCH_3], as obtained from Aldrich Chemical Co., both in the bulk and confined states into sol−gel glasses with modified and unmodified internal surfaces. To confine the bulk liquids, we used GelSil porous glasses with sufficiently high optical quality. The glasses were cylindrical in shape (10 mm diameter, 5 mm thick for light scattering measurements and 5 mm diameter, 1 mm thick for neutron scattering measurements), produced by the sol−gel technology and purchased from GelTech Co. with nominal pores of diameters of 26 Å (5% standard deviation), pore volume fractions of 0.39, surface areas of 609 m^2/g of the glass, and bulk densities of 1.2 g/cm^3.[6] The pores in the glasses are highly branched and interconnected in a fractal-like geometry. The used sol−gel porous glasses (GelSil) contain, on the surface, a great number of SiOH groups, strong active sites for H-bond interaction with the OH groups of the liquid samples. The GelSil glasses were immersed in 30% H_2O_2 and heated to 90 °C for a few hours to

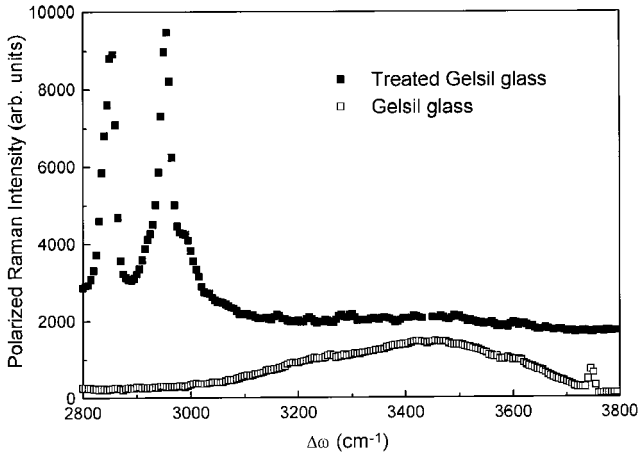

Figure 1. Raman spectra of GelSil glass before and after the chemical treatment with methanol.

remove any organic impurities absorbed by them. They were then washed several times in distilled water in order to remove the hydrogen peroxide. Afterward, they were gently dried under vacuum at room temperature. After this cleaning the GelSil pieces were immersed in the samples under investigation for a sufficient time (3−4 h). It was possible to chemically treat these glasses, using methanol to replace the hydrogen atom of the silanol groups SiOH with the nonactive CH_3; this substitution gives a more hydrophobic inner surface because of the interaction minimization with the fluid molecules. To check the effectiveness of the removal of the hydroxyl groups, we compared the 2800−3800 cm^{-1} region of polarized (VV) Raman spectra before and after the alcohol treatment as shown in Figure 1. The bottom spectrum, obtained for a nontreated sample does not show any trace of methyl groups (CH_3) and a large band centered at ∼3400 cm^{-1} is due to OH-stretching of SiOH groups. The upper spectrum is referred to the same sample after boiling methanol, the strong peaks are assigned to C−H stretching and bending modes of the methoxy groups, whereas no spectroscopic evidence exists for the appearance of the OH-stretching band. In the case of water, to get measurements at various hydration percentage, GelSil was first fulfilled by immersing it in water inside an optical cell for a sufficient time and then outgassed by a vacuum pump, at room temperature for different outgassing times τ_p in the range $60-2.02 \times 10^5$ s. Before each run, the sample was kept at rest for about 6 h to guarantee mechanical and thermodynamical stabilization, as tested by the constancy of the scattered intensity, continuously monitored. For estimating the water amount dispersed within pores, we have simply connected the Raman scattered intensity I^{OH} (integrated in the 2800−3800 cm^{-1} range) to the number N of water scatterers in the scattering volume. The ratio I^{OH}/I_0^{OH} (where I_0^{OH} is the scattered intensity for total filled pores, taken at $\tau_p = 0$) vs τ_p follows an exponential decay (see Figure 1 in ref 21), $e^{-\alpha\tau_p}$, which is expected if our assumption that I^{OH}/I_0^{OH} is proportional to N/N_0 and then to V/V_0 (V being the outgassed water volume) is reasonable. A simple calculation allowed us to obtain the value of N/N_0 of water adsorbed to the GelSil surface in the first layer (considering the molecular diameter of water ∼3 Å), $N/N_0 = 41.6\%$. This indicates that the data taken for $N/N_0 = 15.4\%$ and for $N/N_0 = 5.9\%$ refer to water bonded to the glass inner surface only in the first layer.

In the case of polymers, GelSil was full filled immersing it in the sample under examination (PG, or PPG, or EG, or EGmE, or EGdE) following the same procedure. For estimating the amount of sample within the pores we weighted the glass before and after the filling procedure. The amount of adsorbed liquids was determined by its density and the pore volume fraction.

B. Optical Data: Light Scattering (Rayleigh Wing and Raman) and IR Absorption. Experimental Setup and Theoretical Background. Rayleigh wing and Raman data were collected by a high resolution, fully computerized Spex-Ramalog 5 triple monochromator, used in a 90° scattering geometry. It has been coupled with an INNOVA 70 Series Ar^+-Kr^+ Ion laser providing 6471 Å line for the exciting source that does not induce strong fluorescence effects due to the glass matrix.

IR spectra were collected, only for the bulk liquids at room temperature, with a Bomem DA8 Fourier transform infrared (FTIR) spectrometer, working with a globar lamp source, a KBr beam splitter, and a DTGS/KBr detector. A sample holder with CaF_2 windows was used, and the apparatus was purged with dry nitrogen. We investigated the CH−OH stretching spectral region (2500−3700 cm^{-1}), with a resolution of 4 cm^{-1}. The IR spectra were normalized for taking into account the effective number of absorbers. It is well-known that the O−H stretching vibration reveals a spread contribution, as is usually expected for H-bonded liquids, indicative of the cooperative character of this vibration. IR and polarized (VV) Raman data were deconvoluted in symmetrical Voigt profiles, ω shifted with respect to the fundamental free O−H stretching vibration.

From a theoretical point of view, it is well-known that Rayleigh wing scattering allows the cooperative nature of molecular diffusion to be tested. It is a powerful tool to investigate relaxation processes on the psec time scale, taking into account the time dependence of the traceless part of the polarizability tensor correlation function.[33] As it has been well established, this quasi-elastic depolarized contribution to the light scattering reflects local fluctuations in the anisotropic part of the polarizability tensor and is due to the time correlation, indicated by $C_\beta^{anis}(k,t)$, of the traceless part of the polarizability tensor fluctuations $\delta\beta_{ij}(k,t)$.[34] Depolarized Rayleigh spectra depend on both self-particle motions and correlated motions of different molecules. In H-bonded liquids, cooperative motions, such as fast orientational relaxations, may become important and, under certain assumptions, the self- and interparticle relaxation times have been related. Depolarized dynamic light scattering in moderately viscous associated liquids can be considered as the result of two principal mechanisms: the collective reorientation of optically anisotropic molecules and a second mechanism arising from "interaction induced" or "collision induced" effects. They give rise, respectively, to the orientational pair correlation (OPC) and to the DID term. The first term, in the case of complex H-bonded systems (as our systems), in which exist different transient extended structures triggered by the hydrogen bond, such as branched associates, rings, large chains, is characterized by a distribution of relaxation times for the rotational motion. This occurrence indicates that the Havriliak−Negami profile,[30] as we will show in our case, can fulfill the experimental data better than the Lorentzian one. This latter, in fact, as it is well-known, reflects a simple decay process corresponding to a well-defined relaxation time. Specifically, the dynamical structure−function $S(k, \omega)$, in turns related to $I_{VH}(k, \omega)$, can be described in terms of the imaginary part of the Havriliak−Negami function:[30]

$$HN(\omega) = -(1/\omega)Im[1 + (i\omega\tau_{HN})^{\alpha}]^{-\gamma} \qquad (1)$$

where τ_{HN} is a characteristic relaxation time at optical wavelengths. α and γ are shape parameters ranging between 0 and 1, which are related to the symmetric α and to the asymmetric

γ line width contributions. The HN*(ω)* reflects, in the frequency domain, a distribution of relaxation times. Much evidence of *strong departure* from Lorentzian behavior is present in the literature on the dynamical behavior of associated liquids such as glass-forming systems (including H-bonded liquids, as in our case). Such a function plays, in the ω-domain, the same role of the well-known Kolrausch−Williams−Watt KWW(*t*) profile $\phi(t) = \exp[-(t/\tau_{KWW})^{\beta}]$ in the time domain that, as it is well-known, seems to be the universal function to which slow relaxations, which occur in complex condensed systems, obey. In literature,[30] a mathematical relation between these two functions, experimentally verified, has been found: $\log [\tau_{HN}/\tau_{KWW}] = 2.6(1-\beta)^{0.5}\exp(-3\beta)$ as far as the characteristic times are concerned, and $\alpha\gamma = \beta^{1.23}$ for the shape parameters. These allow a direct way of transformation from the HN parameters into the KWW ones. The two relevant parameters, i.e., the mean relaxation time $\langle\tau\rangle$ and the width of the relaxational times distribution β are linked to the obtained HN*(ω)* fitting parameters τ_{HN}, α, and γ by the relation $\langle\tau\rangle = (\tau_{KWW}/\beta)\Gamma(1/\beta)$, Γ being the Gamma function. Obviously when, in particular, the *HN*(*ω*) shape parameters are equal to 1, the single Debye exponential time decay is restored and the *HN(ω)* assumes the well-known Lorentzian profile. Finally, the CILS (collision-induced light scattering)[33] contribution is usually written as

$$I^{CILS}(\omega) = F(\omega)\exp(-\omega/\omega_0) \qquad (2)$$

where $F(\omega)$ is a slowly varying function ($F(\omega) \approx \omega^{12/7}$ for Lennard-Jones fluids), approximately constant ($F(\omega) \approx C$) for many liquids. Furthermore, ω_0^{-1} can be considered as a measure of the duration of a collision or could be connected with the average period of the HB vibration of the aggregated species.[35]

As far as IR absorption is concerned, it has been well established[33] that it is induced by the coupling between the electric field of the incident e.m. beam and the permanent electric dipole moment of *i*th molecule μ_i. It is well-known that the resulting IR spectrum is composed by a distribution of absorption vibrational bands given by the following relation:

$$A(\omega) = \sum_{\nu}(\mu^{\nu}q^{\nu})^2 G_{\nu}(\omega + \Omega_{\nu}) \otimes F_{1\nu}(\omega + \Omega_{\nu}) \qquad (3)$$

where q^{ν} is the νth normal coordinate, $\mu^{\nu} = (\partial\mu/\partial q^{\nu})_0$, and the terms G_{ν} and $F_{1\nu}$ represent the convoluted vibrational and rotational contributions centered at the frequencies Ω_{ν}. On these bases, the presence, in H-bond liquids, of the highly anisotropic and directional H-bond, whose energy value ranges between 2 and 6 kcal/mol, leads to several kinds of intermolecular arrangements.[36] Taking into account the several contributions composing the potential energy surface of the H-bond (electrostatic, polarization, charge transfer, dispersion), a strict correlation between the degree of association and the relative population of the local structures is expected, generating, in turn, a different dynamic response: this explains the appearance of peculiar bands according to the number of the possible associative species. These aggregates are dynamically stable, and can be considered as *transient structures*, owing to the continuous breaking and reforming of the H-bond, whose mean lifetime is in the psec time scale. On the basis of the cross-links among the inherent structures, corresponding to the various local minima in the system potential energy, it is possible to explain the spectral variations, for H-bonded liquids, of the IR O−H stretching vibration, that spreads out over a large ω range and changes dramatically in frequency (red-shift), shape, and intensity with respect to the original narrow O−H band centered at ~3630 cm^{-1}. It is a consequence of the existence, for these systems, of an electrical *anharmonicity* in the dipole moment function, other than a mechanical one that enters in the potential energy evaluation, which contributes to all nonlinear terms in the dipole moment calculation. It has been well established,[37] in fact, that H-bonded systems hold an exceptional position in vibrational spectroscopy, since the first derivatives of the dipole moment μ with respect to the coordinates of motions $\partial\mu/\partial q_i$ is improper for the prediction of intensities *I*. This means that the familiar relationships $I = K(\partial\mu/\partial q_i)^2$ that usually expresses the intensity of an absorption band in the infrared due to the normal mode q_i, in which *K* is a constant that takes into account the number n_i of oscillators involved in it, is no longer valid for strong H-bond, but can be retained true for weak H-bond systems, as are ours. Supposing that the time dependent electrical field is weak (so that its interaction with the stretching mode may be treated perturbatively to first order, and thus in a linear way with respect to the electrical field), theoretical studies of the shape of the high-frequency stretching vibration of hydrogen bonds are performed within the framework of the linear response theory. According to it, the spectral density *I(ω)* of this stretching mode may be obtained by the Fourier transform of the autocorrelation function $G(t) = \langle\mu^{+}(t)\mu(0)\rangle$ of the dipole moment operator μ: $I(\omega) = (1/\sqrt{2\pi})\int G(t)\exp\{-i\omega t\}dt$. What is required to find the spectral density is the knowledge of the autocorrelation function $G(t)$ of the fast mode averaged on some thermal properties. This autocorrelation function will differ according to the fact that the system is considered classically or quantum mechanically, and according to the hypothesis performed on the origin of the relaxation. Two main mechanisms have been considered in our systems: in the first one the fast mode, after excitation, relaxes directly toward the medium, whereas in the last one, it is relaxing via the slow mode to which it is anharmonically coupled.

C. Neutron Data: IQENS and IINS. Experimental Setup and Theoretical Background. Quasielastic (IQENS) and inelastic (IINS) neutron scattering measurements were collected, on water in bulk and confined at different water percentages, at ORPHEE reactor at Laboratoire Léon Brillouin (LLB) using a MIBEMOL tof spectrometer and at Institut Laue-Langevin (ILL) using an IN6 tof focusing spectrometer. As far as MIBEMOL experiment, the parameters were $\lambda_0 = 9$ Å, energy resolution (fwhm) 28 μeV, *Q* range from 0.308 to 1.220 $Å^{-1}$. The corresponding parameters for IN6 were $\lambda_0 = 5.12$ Å, energy resolution (fwhm) 100 μeV, *Q* range from 0.283 to 1.9375 $Å^{-1}$.

In our investigated samples, because of the presence of hydrogen atoms, which possess an high incoherent cross section that dominates the total spectrum, the double differential cross section $\partial^2\sigma_{total}(Q,\omega)/\partial\Omega\partial\omega$ is related only to the incoherent structure factor through the relation:[38]

$$\frac{\partial^2\sigma(Q,\omega)}{\partial\Omega f\omega} = \frac{1}{4\pi}\frac{|k|}{|k_0|}\sigma_{inc}S_{inc}(Q,\omega) \qquad (4)$$

where $Q = |k - k_0|$ is the exchanged wave vector, and $\sigma_{inc} = 4\pi b_{inc}^2$ is the incoherent scattering function. On the other hand, it is well-known that $S_{inc}(Q,\omega)$ is the Fourier transform of the Van Hove self-correlation function representing the probability that any particle is moved by *r* within the time *t*. Generally speaking, in the quasi-elastic region the spectrum is dominated by diffusive (translational and rotational) atoms motions whereas at high-ω to $S_{inc}(Q,\omega)$ contributes the vibrational density of states $g^{N}(\omega)$.

III. Outlook and Discussion

A. Water. As first results,[25] we present a light scattering analysis of the vibrational dynamics of liquid water, in bulk and in the confined state, in two different regions: (a) the intramolecular O−H stretching region ($2800 < \omega < 3700$ cm^{-1}) and (b) the intermolecular or "restricted translational" O···H stretching and bending region ($0 < \omega < 500$ cm^{-1}).

(a) The Intramolecular Region. To obtain information on the effects of the porous matrix on the HB network of water, we analyze the intramolecular O−H stretching spectral region.

Some years ago, the existence of an isosbestic point in the isotropic spectra of pure water has been explained[39] in terms of two competitive classes of OH oscillators with opposite temperature dependence and has suggested, to some of the present authors, the decomposition of each spectrum into an "open" and a "closed" contribution. The first one has been attributed to the O−H vibration in tetrabonded H_2O molecules that have an "intact bond" and originate low-density patches in the system, while the second one would correspond to the O−H vibration of H_2O molecules that have a not fully developed HB (distorted bond). The "open" component is centered near 3210 cm^{-1}, while the "closed" one is centered near 3420 cm^{-1}. With declining temperature, one finds that the "open" contribution increases indicating an enhanced hydrogen bonding which gives rise to patches of cathalizing four bonded water molecules. A different approach of the OH stretching contribution, which however furnishes almost similar information, includes a spectral stripping procedure of the polarized O−H stretching band and has been suggested by Green, Lacey, and Sceats[40] (GLS). More specifically, GLS proposed that the low-frequency shoulder in the I_{VV} spectrum of H_2O arises from "collective" modes of the OH groups. The collective band is essentially that part of the spectrum characterized by a depolarization ratio which differs from that of uncoupled OH oscillators. Coupling of OH oscillators gives rise to a strongly polarized band on the low-frequency edge of the spectrum. To obtain the relative intensity of this mode, it is assumed that the I_{VH} spectrum looks basically like the scaled-down version of the I_{VV} spectrum without the collective band I_C. Then I_C can be obtained by subtracting, after an appropriate data reduction, I_{VH} from I_{VV}. After this stripping procedure, the fractional collective band intensity, in pure water, was shown to increase linearly with falling temperature and to approach the value of ice at the singularity temperature of water ($T_s = 218$ K). GLS have conjectured that this collective band arises from the collective in-phase stretching motion of the water molecules in the *fully bonded tetrahedral network*, to which liquid water tends as it is supercooled. Other studies on aqueous solutions have shown that the presence of "defects", broadly identifiable as broken HBs, reduces the collective band intensity.[40] In Figure 2A the polarized (VV) and depolarized (VH) Raman spectra in bulk water (spectra a) and in water confined in GelSil (spectra b and c) are reported. The streaking feature is the clear falling down of the collective contribution (its center frequencies are localized by the dashed arrow) with the decrease of the water content. The result of such a stripping procedure is reported in Figure 2B, which shows the collective band for various values of N/N_0. For bulk water this contribution closely remembers the *open* water contribution as shown in ref 39. The behavior suggests that the GelSil matrix promotes a *destructive effect* on the tetrahedral H-bond network of pure water.

(b) The Intermolecular Region. Figure 3A shows the experimental Rayleigh wing spectra of pure water and, as an example, (a) in water in GelSil at $N/N_0 = 5.9\%$ together with (b) the

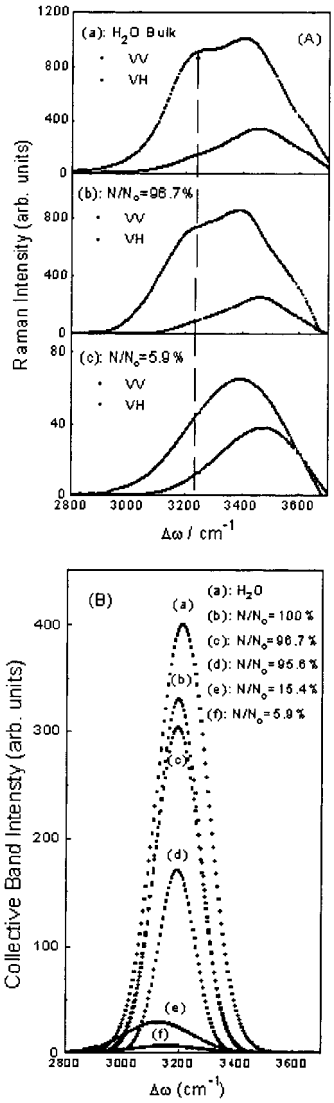

Figure 2. Polarized (VV) and depolarized (VH) OH stretching (A) Raman intensity and (B) collective band intensity for bulk and confined water at different relative percentages N/N_0.

theoretical fit performed using the following scattering law:

$$I_{VH}(\omega) = \mathrm{Res}(\omega) + HN(\omega) + Vgt_1(\omega) + Vgt_2(\omega) + Bkg \quad (5)$$

where Res(ω) represents the resolution enlarged Gaussian contribution, HN(ω) represents the imaginary part of the above-described Havriliak−Negami profile, $Vgt_1(\omega)$ and $Vgt_2(\omega)$ are Voigt profiles, and *Bkg* is a flat background that takes into account the dark count level and the flat fluorescence signal. Table 1 shows the HN(ω) best-fit parameters for all the investigated samples in bulk and in the confined state. In pure water the HN(ω) profile is close to the Lorentzian[41] profile ($\tau_{HN}/\langle\tau\rangle \approx 1$, $\beta \approx 1$). The HN(ω) contribution can be interpreted as the analogous of the fast contribution of ref 41. Its origin can be due to the motion of water into the various transient cages HB imposed. These latter give rise to a multiplicity of the above-mentioned primary elemental rates, i.e., to the obtained distribution of relaxation times. Furthermore, we observe a systematic increase of the $\langle\tau\rangle$ with the decrease of the amount of water, which can be connected with the existence of both *chemical* and *physical* traps. At the same time, we observe a decrease of β from 0.88 (pure water) to 0.64 (fully adsorbed water). The

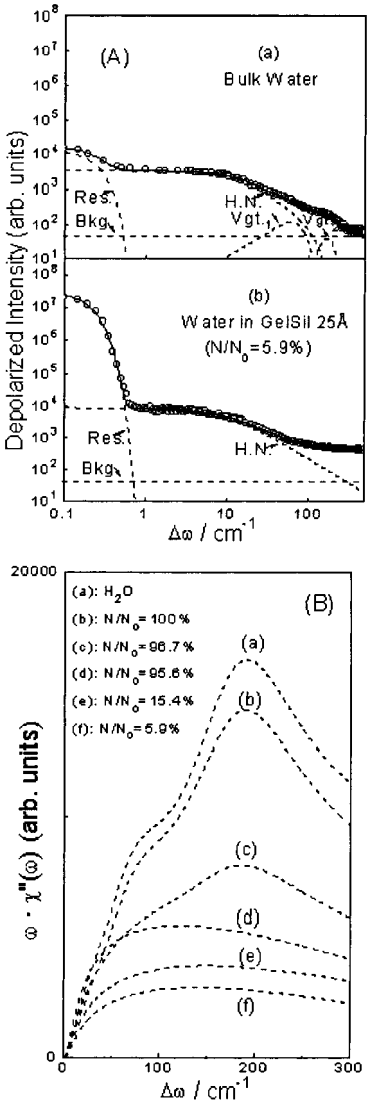

Figure 3. (A) Rayleigh wing spectra and (B) Raman effective VDOS of bulk and confined water.

evolution of these two relevant parameters calls for a justified hypothesis: first, it seems that, as expected, HB between glass surface and water is energetically stronger ($\langle\tau\rangle$ increases) respect to what is observed among water molecules; second, the variation of $\langle\tau\rangle$ distribution width (β increases) could correspond to the existence of a larger number of new different transient species, imposed by the existence of interfacial HB, respect to the those existing in liquid water. Finally, the Voigt bands, centered at 60 and 170 cm^{-1}, identified as HB bending (the lowest one) and HB stretching lattice modes, *disappear* starting from $N/N_0 = 95.6\%$; so only the HN(ω) contribution is still present.

If a solid state point of view is assumed for explaining the restricted translational region spectra, the data can be reduced for obtaining the effective susceptibility $\chi''(\omega)$, given by $\chi''(\omega) = I_{VH}(\omega)(n(\omega,T) + 1)^{-1}$, where symbols have the usual meaning and $n(\omega,T) + 1$ is the well-known Bose−Einstein population factor. From $\chi''(\omega)$ is then possible to obtain the effective Raman vibrational density of states: $g^R_{eff}(\omega) = \omega\chi''(\omega)$. We have evaluated $g^R_{eff}(\omega)$ and the results are shown in Figure 3B for various confined water concentrations. Experimental results for pure liquid water at $T = 20$ °C agree well with the VDOS recently obtained in a MD simulation.[42] In Figure 3B, $g^R_{eff}(\omega)$ for pure water (a), induced by localized vibrational excitations of the molecules, reveals the two above-mentioned characteristic bumps, the first one convoluted with the acoustical like contribution. Furthermore, we observe that the $g^R_{eff}(\omega)$ changes dramatically by lowering the content of water (curves b−f) confined in the porous matrix, giving rise to a flattening of the spectral profile, in which the symmetries proper of pure water are lost, the interactions among water molecules and active Si−OH surface groups destroying the intermolecular network of water.

Concerning IQENS measurements, we report, extracting from the data collected by MIBEMOL and IN6, a set of results in the case of confined water at different temperatures. The data have been fitted with two different scattering laws. The first one is based on the Dianoux-Volino model for the confined diffusion,[43] in which the dynamic structure factor from the hydrated sample is written as

$$S(Q,\omega) = e^{-\langle u\rangle^2 Q^2/3}\left[A(Q)\delta(\omega) + \frac{(1 - A(Q))}{\pi}\frac{\Gamma(Q)}{\omega^2 + \Gamma^2(Q)}\right] \otimes \mathrm{Res}(\omega) + bkg \quad (6)$$

as can be seen, the spectral line shape for this case is the weighted superposition of an elastic (δ function) and a quasi-elastic peak (Lorentzian in character). The Q-dependent factor $A(Q)$ is the elastic incoherent structure factor (EISF), identical to the form factor of the confining volume. An analytical expression of the EISF for a particle confined in a spherical volume of radius a can be written as

$$A(Q) = \left[\frac{3j_1(Qa)}{Qa}\right]^2 \approx \exp\left[-\frac{1}{3}Q^2a^2\right] \quad (7)$$

As far as spectra collected on MIBEMOL are concerned,[44] Figure 4A,B shows, as an example, the behavior in the case of confined water at $T = -25$ °C, $T = -10$ °C and $T = 1$ °C, of the line width Γ vs Q for the Lorentzian contribution and the EISF intensity vs Q, together with a fit that furnishes a dimension of the cage $d^* = 2\pi Q^{*-1}$. In our case the dimension of the cage turns out to be $d^* \sim 8$, ∼9, and ∼13 Å for $T = -25$, −10, and 1 °C, respectively. Also the spectra collected at IN6 for bulk and confined water at different temperatures and different hydration percentages were first fitted in the framework of Dianoux−Volino model, but adding another Lorentzian line reflecting the rotational contribution, not seen by MIBEMOL because of the more limited spectral Q range (0.308−1.220 $Å^{-1}$) with respect to the one spanned by IN6 (0.283−1.9375 $Å^{-1}$). Figure 4C reports, as an example, the best fit in the case of fully hydrated water at $T = 20$ °C, and Figure 4D, the behavior of $\Gamma(Q)$ for the narrow Lorentzian contribution at all the analyzed temperatures.

The second model[26] is based on the presence of an α-relaxation process in water that, at low T, leads to a slow dynamics recalling the MCT relaxation process of the kinetic glass transition in dense supercooled liquids. This model hypothesizes the presence of a distribution of relaxation times for the density correlation function (KWW empirical law). We have fitted the quasi-elastic spectra by the HN(ω) distribution function convoluted with the resolution contribution

$$S_s(Q,\omega) = [\mathrm{HN}(\omega)]\otimes\mathrm{Res}(\omega) + bkg \quad (8)$$

In Figure 5 the resulting parameter, $\langle\tau\rangle$ vs Q, obtained in the case of MIBEMOL data, is represented. As can be seen, $\langle\tau\rangle$, in the Q range explored, has a power-law dependence, $\langle\tau\rangle \approx Q^{\gamma'}$.[26]

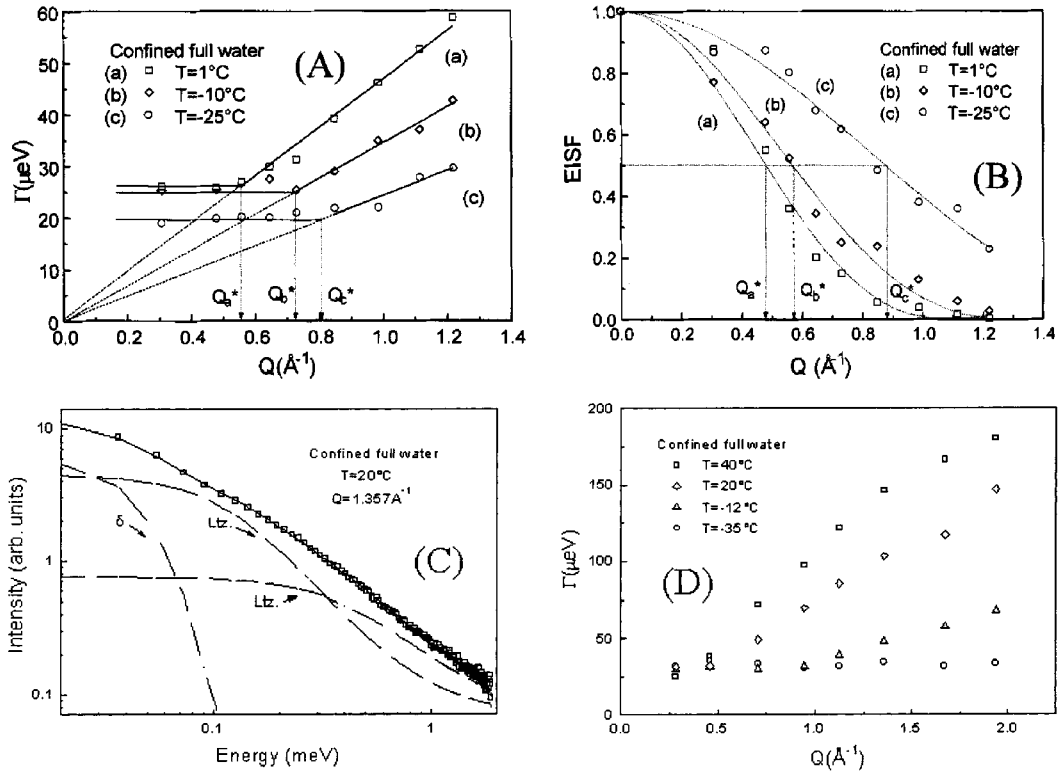

Figure 4. (A, B) MIBEMOL and (C, D) IN6 neutron data analysis for confined full water at different temperature according to Dianoux−Volino model.

TABLE 1: Rayleigh Wing Best-Fit Parameters for All the Analyzed Samples

		Negami					experimental	Ltz
environment	sample	τ_{HN}(ps)	α	γ	β	$\langle\tau\rangle$ (ps)	τ_{exptl} (ps)	τ_{Ltz} (ps)
bulk	H_2O	0.31	0.97	0.88	0.88	0.3		
	PG	2.5	0.9	0.9	0.84	2.3	0.1	
	PPG 425	3.1	0.85	0.9	0.73	2.7	0.1	
	PPG 725	3.8	0.8	0.8	0.7	3.2	0.1	
	PPG 4000	4.7	0.8	0.75	0.66	3.9	0.1	
	EG	3.8	0.9	0.39	0.42	5.2	0.09	
	EGmE	2.9	0.97	0.44	0.5	3.8	0.1	
	EGdE	1.8	1	1	1	1.8	0.1	
in unmodified GelSil 25 Å	H_2O, 100%	0.42	0.72	0.77	0.62	0.5		
	H_2O, 96.7%	0.44	0.80	0.77	0.67	0.5		
	H_2O, 95.6%	0.50	0.93	0.75	0.75	0.5		
	H_2O, 15.4%	0.53	0.93	0.65	0.66	0.6		
	H_2O, 5.9%	0.55	0.96	0.60	0.64	0.6		
	PG	2.7	1.0	1.0	1.0	2.7		0.1
	PPG 425	4.0	1.0	1.0	1.0	4.0		0.1
	PPG 725	4.4	1.0	1.0	1.0	4.4		0.3
	PPG 4000	6.3	1.0	1.0	1.0	6.3		0.1
	EG	5.8	0.99	0.78	0.81	6.0		0.1
	EGmE	4.8	0.99	0.69	0.73	5.0		0.1
	EGdE	4.0	1	1	1	4.0	0.1	
in modified GelSil 25 Å	PG	2.5	0.9	0.9	0.84	2.3	0.1	
	PPG 425	5.0	0.85	0.85	0.77	4.4	0.1	
	PPG 725	6.0	0.8	0.8	0.7	5.1	0.2	
	PPG 4000	6.5	1.0	1.0	1.0	6.5		0.1
	EG	4.0	0.5	0.8	0.47	5.4	0.1	
	EGmE	4.3	0.5	0.98	0.56	5.8	0.1	
	EGdE	4.0	1	1	1	4.0	0.1	

We obtain γ' values definitively less than two (confinement effect) and diminishing when T decreases. Furthermore, β tends to 1 (inset of Figure 5) for diminishing temperatures indicating, in our opinion, that the single relaxation decay tends to be restored, due to a decreasing of the transient species population distribution induced by a weaker influence of thermal destructing energy K_BT.

As far as vibrational dynamics is concerned, we performed, on the same samples previously analyzed by IQENS, IINS experiments at IN6. We obtained the proton weighted VDOS $g^N(\omega)$ following the reduction method as applied in ref 32 with the multiphonon contribution calculated and subtracted. $g^N(\omega)$, in the case of fully hydrated water (crosses) and partially hydrated water (circles), at $T = -35$ °C, are shown in Figure 6, where the disappearance of the tetrahedral intermolecular stretching mode at ∼25 meV and a dropping of the one (bending

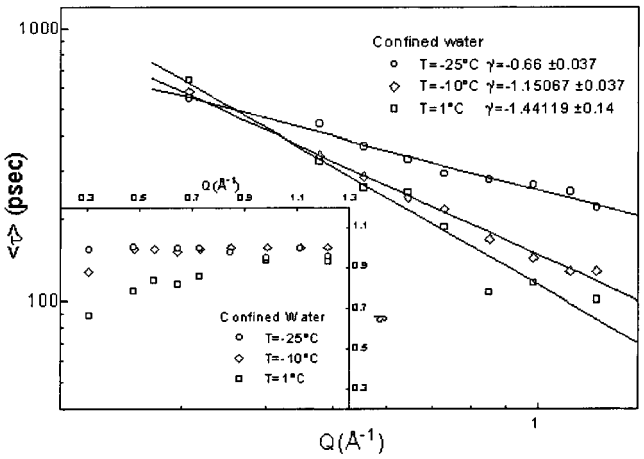

Figure 5. $\langle\tau\rangle$ vs Q and, in the inset, β vs Q for confined water at $T = -25, -10, 1$ °C.

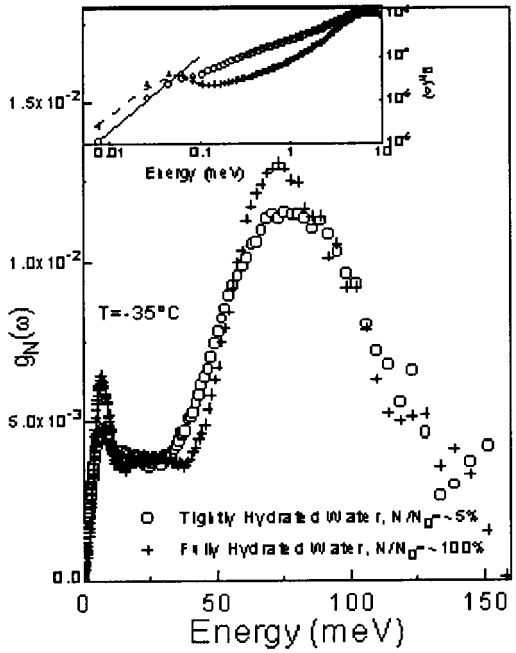

Figure 6. IINS experimental results for (cross) fully and (open) partially hydrated water.

mode) at ~8 meV is clearly evident for partially hydrated water, confirming the results obtained by P. Gallo et al.[17] by means of MD simulation of water in 40 Å diameter pores of Vycor glass and by M. C. Bellissent-Funel et al.[26] by IQENS in the same matrix as well, and finally by our group too[25] analyzing the above examined Rayleigh wing data. Furthermore, the librational band (large bump centered at about 80 meV) shifts at higher frequency for partially hydrated water. In the same figure the inset shows the behavior of the very low-frequency acoustical contribution to the $g^N(\omega)$. The two observed slopes recall, in fully hydrated water, the familiar ω^2 law superimposed to a definitive peak recalling a boson peak[17] and in partially hydrated water a fractal-like behavior $\sim w^d$ ($d < 2$).

B. PG and Its Oligomers. In the PG molecules and their oligomers,[24] H-bond promotes a set of transient cross-links between neighboring molecules, originating relevant transient structures such as branched associated species and/or chains. As in the case of ethylene glycol, many conformations can be generated for each molecule by the rotation of the CH_2-OH group around the $C-C$ axis in respect to the $OH-CH(CH_3)$ group. In particular, a computer simulation in the case of an isolated PG molecule shows that a gauche form, stabilized by an intramolecular H-bond, has a high probability of existence. On the ground of above observations and by taking into account that we are in the presence of molecular anisotropic liquids, Rayleigh wing spectra, in bulk liquid samples, are due to a collisional induced contribution (CILS term), reflected in the far wing. This contribution is generally originated by the molecular frame distortion during collisions, in which one of the colliding molecule can be identified, in the case of pure PG, with the free molecule in the gauche form. A further contribution is the previously described Havriliak−Negami profile, that can be connected with the existence of *different transient extended* structures triggered by the H-bond. The experimental Rayleigh wing spectra in the case of bulk PG and its homologous systems were fitted by using the following scattering law:

$$I_{VH}(\omega) = R(\omega) + \mathrm{HN}(\omega) + I^{CILS}(\omega) + B \qquad (9)$$

where, other than the already described line shapes, $R(\omega)$ represents the nonresolved very narrow contribution (Gaussian line), that could be induced by unwanted parasitic light non completely rejected by the polarizer, and B is a very small flat background. The dependence of the fit parameters by the polymers' molecular weight for the liquid polymers is reported in Table 1. By an inspection, it results evident that $\tau_{CILS} < \tau_{HN}$ for all investigated bulk samples and β diminishes by increasing molecular weight. Such a behavior verifies the hypothesis that different molecular entities are involved in *simultaneous parallel dynamical events*. In particular, the fastest process takes origin from a gaslike collisional behavior while the slowest depends on the relaxation of the local order imposed by the H-bond.

The depolarized quasi-elastic data for confined systems in unmodified matrix were fitted by

$$I_{VH}(\omega) = R(\omega) + \mathrm{HN}(\omega) + L(\omega) + B \qquad (10)$$

The confined liquids loose, in the far wing, the collisional effect (fluid like) as a consequence of a sort of freezing effect, giving rise to a very fast (~0.1 ps) relaxation process (Lorentzian in character), in agreement with prediction of Wang and Wright's model.[35] The crossover from exponential decay (CILS) to Lorentzian one (collective relaxation) was already detected by incoherent quasi elastic neutron scattering on water in porous matrix of polyelectrolyte gels of different pores size:[45] the water single-particle diffusive modes die out and only collective modes remain active as the dimension of pores reaches the value of 25 Å (microspace effect). Therefore, one may expect a progressive crossover to an essentially collective dynamics in confined associated liquids, as the size of the inner pore volume approaches the dimension of hydrogen bonded clusters. In this case it has to be noticed that the HN(ω) function shapes parameters α and γ are equal to 1 ($\beta = 1$) indicating that a Lorentzian shape is recovered. This behavior can be rationalized because of a retardation effect of the molecular mobility, essentially driven by the trapping of the hydrogen bonded clusters at the surface. In addition, purely geometrical restrictions are present, which strongly reduce the possibility of existence of different aggregates. In particular, we hypothesize that only linear *end to end* type associates survive, responsible of the collective reorientational relaxation detected. The Rayleigh wing analysis of the confined polymers in inert porous glass shows very interesting features, as reported in Table 1. Low molecular weight samples (PG, PPG 425, PPG 725) can be described by means of the eq 9. In such a case a distribution of relaxation

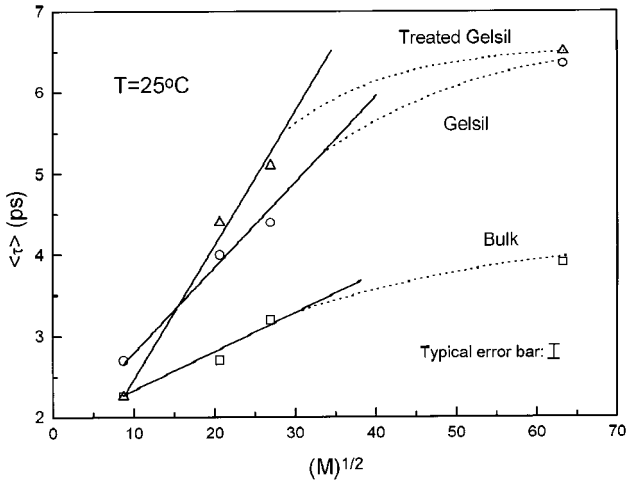

Figure 7. $\langle\tau\rangle$ vs MW for (squares) bulk and (circles) confined PPGs in unmodified and (triangles) modified GelSil.

times ($\beta < 1$) is also revealed. It is closely related to the absence of *chemical traps* on the inner surface of the porous glass and it causes a dynamical behavior similar to the one observed in the bulk. On the other hand PPG 4000 can be fitted with the scattering law of eq 10. In this case the long chain, length (∼47 Å) enhances the effect of the *physical traps*, thus limiting the allowed configurations. In Figure 7 we report the MW dependence of $\langle\tau\rangle$ for bulk and confined polymers, in both non modified and modified GelSil. As it can be seen at low molecular weight, the polymers show a roughly $M^{1/2}$ dependence, indicating a mass-dependent scaling effect. For the monomer the same value of $\langle\tau\rangle$ for the bulk and for PG in modified glass is obtained, indicating that the *physical traps* are not important. In such a case, in nonmodified GelSil, *chemical traps* are more efficient in retarding the rotational motion. In the limit of high molecular weight, $\langle\tau\rangle$ is the same in the modified and nonmodified Gelsil, indicating that the *chemical traps* play a minor effect on the studied dynamics and the geometrical confinement plays the major role. Finally the higher value of $\langle\tau\rangle$ for oligomers in modified GelSil with respect to the value for unmodified glass, is related to the further lowering of the available space as a consequence of the substitution of the small H atom with the CH_3 unit. In fact in such a case the effective section, for the reorientation processes, of the cylindrical pores decreases of about 10% of the total, causing a more hindered diffusive dynamics.

C. EG and Its Homologous. To separate the effects of chemical and physical traps in the confined dynamics we analyzed, on the bulk and confined state, liquid EG and its homologous systems, EGmE and EGdE, characterized by a different number of OH end groups per molecule, namely, *two* for EG, *one* for EGmE, and *zero* for EGdE.[23] The noticeable importance of EG, that is, the monomeric unity of poly(ethylene oxide) (PEO), is linked to its possibility in forming H-bonded intramolecular interactions other than the intermolecular ones.

Concerning IR and Raman measurements, as referred in section I, IR and Raman spectroscopies give a direct evidence of the intermolecular interactions presence in associated liquids (alcohols, carboxylic acids, and our samples), through the analysis of the vibration that suffers the interactions (in our case sites OH and hence OH stretching region (3000−3800 cm^{-1})). In this way, as above stressed, is convincingly possible to justify the application of particular shapes (for example, the H−N profile) for the scattering law for the Rayleigh wing data analysis. Laubereau and co-workers[36] carried out, in a time-resolved infrared spectroscopy study, an authoritative analysis (in alcohols) of the connection between the local environment of H-bonded molecular groups and the O−H stretching shape. According to this formalism, we indicated with ω_α the fundamental O−H stretching mode of free and/or end groups, ω_β (ω_γ) the O−H stretching of proton-acceptor (donor) end groups corresponding to dimeric structures. Keeping on, ω_δ is referred to the O−H intramolecular stretching vibration corresponding to a condition in which both oxygen and hydrogen are involved in intermolecular H-bond with neighboring unities generating trimers. Finally, we defined ω_ϵ as the vibration of OH groups involved in intramolecular H-bonds of monomeric closed structures. This type of analysis has been previously and successfully applied by our group in the case of bulk EG and its oligomers PEGs,[46] as well as in the case of PG and PPGs,[24] with varying molecular weight. In particular, for the former, we assigned the band centered at ∼3200 cm^{-1} to the ω_ϵ O−H vibration, the one centered at ∼3350 cm^{-1} to the ω_δ O−H vibration and, finally, the band centered at ∼3500 cm^{-1} to the ω_γ O−H vibration. A similar procedure has been used in order to explain IR data for all investigated samples in the bulk state, deconvolving the O−H band into symmetrical Voigt profiles. In this way we observed (Figure 8A) three subbands, $\omega_\epsilon \sim 3207$ cm^{-1} (with a relative percentage intensity $I_\epsilon \sim 48.09\%$), $\omega_\delta \sim 3367$ cm^{-1} ($I_\delta \sim 26.01\%$), and $\omega_\gamma \sim 3479$ cm^{-1} ($I_\gamma \sim 25.9\%$) for EG, and two subbands $\omega_\delta \sim 3351$ cm^{-1} ($I_\delta \sim 72.14\%$) and $\omega_\gamma \sim 3461$ cm^{-1} ($I_\gamma \sim 27.86\%$) in the case of EGmE. No peaks have obviously revealed in the case of EGdE in the O−H stretching region, not being an H-bonded liquid. In Figure 8A, the C−H stretching region (2500−3000 cm^{-1}) is also shown. For all investigated systems, the nonappearance of the ω_α and/or ω_β bands indicates the absence of end and/or open monomers, being almost all the hydroxyl O−H groups involved in inter- and intramolecular H-bond interactions. As far as EG is concerned, the existence of a large variety of aggregates, namely, closed monomeric structures together with dimeric and trimeric aggregates, is closely related to the dimension of the chain and to the presence, in its chemical structure, of two terminal hydroxyl groups. It has to be noticed that the band centered at 3207 cm^{-1} ω_ϵ, connected to the intramolecular O···H bond, disappears in EGmE. It could be due to the different chemical structure: this system presents only one hydroxyl end group and so there is no possibility to organize the intramolecular H-bond. As it appears clear from the analysis of the obtained spectra, we observed, also in this case, the O−H stretching peaks corresponding to dimeric and trimeric units, indicating that the steric hindrance linked to the different structure of the molecule is not sufficiently great to avoid polymeric aggregates of coordination numbers three or four, existing in liquid phase. As far as Raman measurements are concerned, the band shape analysis of highly polarized OH Raman bands is a well established and widely used method to study vibrational properties in liquids. As in the case of IR answers, the analysis of the O−H stretching vibration gives information about the environments of this molecular group.[46] It happens because the spectroscopic features of this band can be explained in terms of different positions of the hydroxyl group inside the molecular arrangements. For example, the O−H end group center frequency differs from that of the hydroxyl group sited in an internal position. Because in our case the experimentally obtained data result highly polarized, to interpret our data we have analyzed only the polarized (VV) spectra. We applied, for our systems in the bulk state and in the confined one, the same model as in the case of IR measurements. In fact, as it

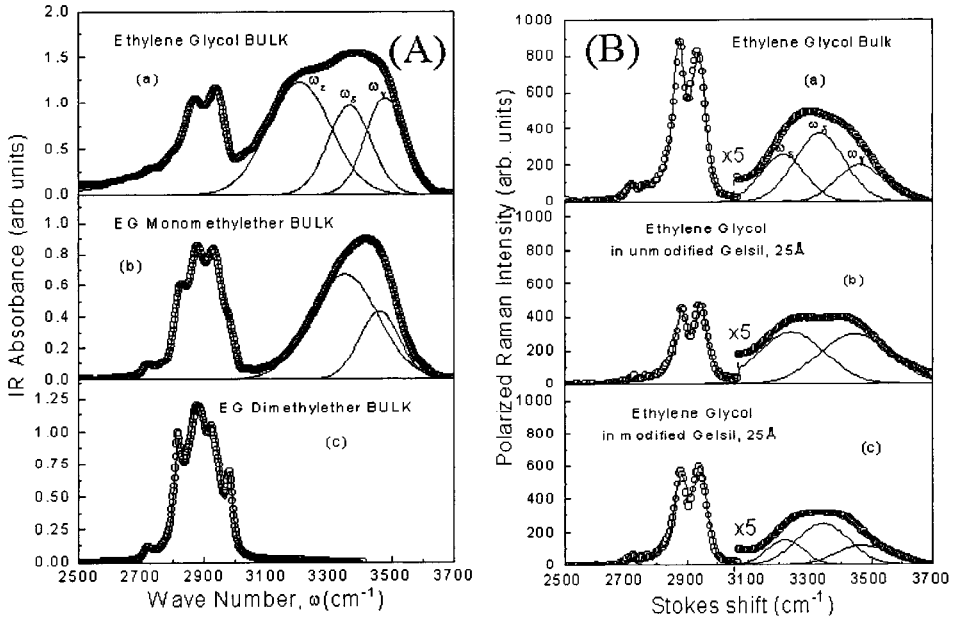

Figure 8. IR data for (A) bulk samples and, as an example, (B) Raman data for bulk and confined EG.

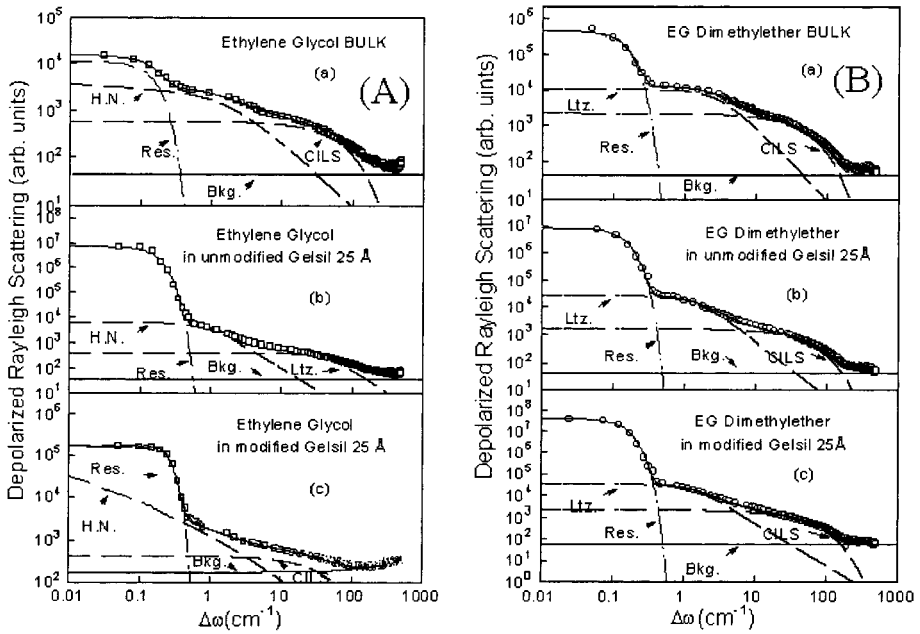

Figure 9. Rayleigh wing spectra for bulk and confined (A) EG and (B) EGdE.

was expected, all the experimental data exactly confirm the results obtained for the IR spectra and previously justified. Figure 8B shows, as an example, the deconvolution of O−H stretching region in the case of EG bulk ($\omega_\epsilon \sim 3223$ cm^{-1} with $I_\epsilon \sim 28.77\%$, $\omega_\delta \sim 3343$ cm^{-1} with $I_\delta \sim 47.94\%$, and $\omega_\gamma \sim 3473$ cm^{-1} with $I_\gamma \sim 23.29\%$) and confined in unmodified ($\omega_\epsilon \sim 3250$ cm^{-1} with $I_\epsilon \sim 48.56\%$ and $\omega_\gamma \sim 3455$ cm^{-1} with $I_\gamma \sim 50.44\%$) and modified ($\omega_\epsilon \sim 3225$ cm^{-1} with $I_\epsilon \sim 22.23\%$, $\omega_\delta \sim 3347$ cm^{-1} with $I_\delta \sim 53.27\%$, and $\omega_\gamma \sim 3470$ cm^{-1} with $I_\gamma \sim 24.5\%$) GelSil glass. Its results are evidence that, in the case of EG bulk and confined in modified GelSil, the different aggregates are the same, probably due to the presence of the *physical* traps only that do not affect the kinds of structural arrangements present in the bulk. Instead in the case of unmodified GelSil the disappearance of trimers (ω_δ) could be related to the presence of the *chemical* traps between the inner surface of the pores and our systems that hinder the subbands linked to more extended species present in the bulk.

On the basis of IR and Raman measurements, which reveal the presence of different structural aggregates, we can explain the obtained results in the case of Rayleigh wing measurements. For the two H-bonded bulk liquids, EG and EGmE, the following main contributions in the Rayleigh wing result (see Figure 9A, spectra a, as an example): (i) a slow zero- frequency centered component that takes into account a distribution of relaxations in the ω-domain and (ii) a collisional induced contribution (CILS). Then we used the same scattering law as in the case of bulk PPGs.

In the case of bulk EGdE (see Figure 9B, spectra *a*), which could behave as a molecular noninteracting liquid, the used fitting law is described by the following form:

$$I_{VH}(\omega) = R(\omega) + L(\omega) + I^{CILS}(\omega) + B \qquad (11)$$

where a Lorentzian line $L(\omega)$ takes the place of the HN(ω) profile for which $\alpha = \gamma = \beta = 1$, as it is expected in the case

of a nonassociated liquid because of the presence of a single Debye exponential time decay.

For EG (Figure 9A, curve *b*, as an example) and EGmE confined in unmodified GelSil, the depolarized quasi-elastic spectra have been fitted by the same law used in the case of confined PPGs in unmodified glass. Also in this case, $L(\omega)$, which describes the far wing contribution, provides a fast time decay of ~0.1 ps (Table 1), justified in the framework of Wang and Wright's model.[35]

EGdE confined into unmodified glass (Figure 9B, curve b) follows the fit law (11) held for the bulk, showing that the presence of *physical* traps affects its dynamics only slowing down it (see Table 1).

Finally, by an inspection of Table 1, which contains the best-fit parameters for all investigated samples in bulk and in the confined state, it is clear a systematic dependence of the dynamic behavior monitored by Rayleigh wing spectroscopy on the number of hydroxyl groups. In fact, in the bulk EG, a distribution of relaxation times (corresponding to a distribution of structures) has been revealed, having $\langle\tau\rangle = 5.18$ ps and $\beta = 0.42$. IR and Raman data have already confirmed these features. When the sample is confined in unmodified silica gels of 25 Å diameter pores, the two hydroxyl groups per molecule of EG present in the interfacial layer cause a more rigid coupling of the system to the surface. We observed, due to the H-bond that EG molecules induce with the active silanol group Si−OH on the inner surface, a slowing down of the reorientational dynamics with respect to the bulk one because of both *chemical* and *physical* traps existence. A distribution of relaxation times, corresponding to the existence of different transient species, is present, and from the best-fit data we obtained $\langle\tau\rangle = 5.92$ ps and $\beta = 0.81$. The higher evaluated value of β and, as a consequence, a narrower distribution, indicate the disappearance of some structural aggregate, as it has been emphasized by analyzing Raman and Infrared spectra in the O−H stretching region.

The confinement of bulk liquids in inert porous glasses leads to really interesting features. The substitution of the proton within the silanol group Si−OH with the nonactive CH_3 group prevents the adsorption of the molecules in the interfacial layer takes place: we expect, hence, for EG, a dynamical behavior similar to the bulk (Figure 9A, curve c). Experimental data indicate a distribution of relaxation times having $\beta = 0.47$, slightly larger than the bulk one, and $\langle\tau\rangle = 5.38$ ps, the dynamics being slowed by the tortuosity of the pores, due to *physical* traps presence that, in this particular case, constitutes the only relevant effect.

EGmE in the bulk and confined state exhibits a behavior analogous to the EG molecule. Geometrical restrictions and surface interactions, acting on the system confined in modified GelSil, give rise to a bulklike reorientational and diffusive dynamics but characterized, in this case, by an increasing value of $\langle\tau\rangle$. This slowing down effect can be justified taking into account the increased steric hindrance, linked to the different structure of the molecules and the restriction of the effective section of the pores owing to the substitution Si−OH → Si−O−CH_3.

Geometrical restrictions play the *only* relevant role for EGdE (Figure 9B, curve c) that, not having any hydroxyl group in its chemical structure, cannot be "trapped" by the H-bond with the inner surface and shows, as a consequence, the same behavior in unmodified and modified Gelsil. It is only possible to deduce a slowing down of the dynamics connected to the *physical* traps. In this case, either in the bulk or in the confined state, it has to be stressed that the HN(ω) function shape parameters α and γ are equal to 1: it implies $\beta = 1$, and as a consequence, a Lorentzian shape is recovered. This has to be expected, because EGdE is not an H-bonded liquid and so the formation of any kind of intermolecular arrangement results impossible.

IV. Concluding Remarks

In this paper we have put into evidence some of the most meaningful results of a detailed analysis of the structural and dynamical properties of some H-bonded liquids confined in nanoporous glasses, obtained in the past few years by our research group with the employment of IR absorption, Rayleigh wing, Raman, and neutron scattering.

From the data analysis, the following general points result: (i) in the confined samples a frustration in the molecular reorientational dynamics is observed in connection with chemical and physical traps, and the quantitative analysis of the different contributions in the Rayleigh wing spectra gave us the possibility to separate the role played by the active and nonactive surface sites on the diffusive reorientational processes. (ii) In addition, the IR and Raman measurements performed in the OH stretching region allowed us to identify the inter- and intramolecular, H-bond imposed, subbands as well as to connect them to different intermolecular environments originated by the existence of the H-bond potential, according to the current theory of associated liquids. In the case of water this kind of analysis has been particularly stressed, also with the employment of the neutron scattering, to obtain a deeper clarification of its modified structural and dynamical (vibrational and diffusional) properties. For what concerns the diffusional dynamics, it seems that at room temperature in the confined state, the behavior of confined water mimes that of the supercooled state with a frozen effect. Actually for what concerns the structural and vibrational properties, the confinement effects seem to induce strongly destructive effects in the interfacial water, where hydration phenomena give rise to different environments evidenced by new spectral features, and loss of the tetrahedral environments (icelike), characteristic of pure water. This last feature is also clearly revealed in the VDOS spectrum by the IINS experiment. Finally the quasi-elastic neutron response is explained in terms of two available current models: the Dianoux−Volino model and the MCT model.

References and Notes

(1) Klafter, J.; Blumem, A.; Drake, J. M. *Relaxation and Diffusion in Restricted Geometry;* Klafter, J., Drake, J. M., Eds.; Wiley: New York, 1989; p 1.

(2) Migliardo, P. *J. Phys.*: *Condens. Matter* **1993**, *5*, 157.

(3) Carini, G.; Crupi, V.; D'Angelo, G.; Majolino, D.; Migliardo, P.; Mel'nichenko, Y. B. *J. Chem. Phys.* **1997**, *107*, 2292.

(4) Kremer, F.; Huwe, A.; Arndt, M.; Behrens, P.; Schwieger, W. *J. Phys. Condens. Matter*. **1999**, *11*, 175.

(5) Guo, Y.; Langley; K. H.; Karasz, F. E. *Phys. Rev. B* **1994**, *50*, 3400.

(6) Arndt, M.; Stannarius, R.; Gorbatschow, W.; Kremer, F. *Phys. Rev. E* **1996**, *54*, 5377 and references therein.

(7) Onori, G.; Santucci, A. *J. Phys. Chem.* **1993**, *97*, 5430 and references therein.

(8) Giordano, R.; Migliardo, P.; Wanderlingh, U.; Bardez, E. *Phys. B* **1995**, *213*, 585.

(9) Bardez, E.; Giordano, R.; Jannelli, M. P.; Migliardo, P.; Wanderlingh, U. *J. Mol. Struct.* **1996**, *383*, 183.

(10) West, J.; Hench, L. L. *Chem. Rev.* **1990**, *90*, 70.

(11) Mel'nichenko, Y. B.; Schuller, J.; Richter, R.; Ewen, B.; Loong, C. K. *J. Chem. Phys.* **1995**, *103*, 2016.

(12) Dozier, W. D.; Drake, J. M.; Klafter, J. *Phys. Rev. Lett.* **1986**, *56*, 197.

(13) Borisov, B. F.; Charnaya, E. V.; Kumzerov, Yu. A.; Radzhabov, A. K.; Shelyapin, A. V. *Solid State Commun.* **1994**, *92*, 531.

(14) Won, A. P. Y.; Kim, S. B.; Golgburg, W. I.; Chan, M. H. W. *Phys. Rev. Lett.* **1993**, *70*, 954.

(15) Soper, A. K.; Bruni, F.; Ricci, M. A. *J. Chem. Phys.* **1998**, *109*, 1486.

(16) Steytler, D. C.; Dore, J. C.; Wright, C. J. *Mol. Phys.* **1983**, *48*, 1031.

(17) Spohr, E.; Hartnig, C.; Gallo, P.; Rovere, M. *J. Mol. Liq.* **1999**, *80*, 165. See also Gallo, P.; Rovere, M.; Ricci, M. A.; Hartnig, C.; Spohr, E. *Philos. Mag. B* **1999**, *79*, 1923.

(18) Liu, G.; Li, Y.; Jonas, J. *J. Chem. Phys.* **1991**, *95*, 6892.

(19) Korb, J. P.; Malier, L.; Cross, F.; Xu, S.; Jonas, J. *Phys. Rev. Lett.* **1996**, *77*, 2312.

(20) Loughnane, B. J.; Scodinu, A.; Fourkas, J. T. *J. Phys. Chem. B* **1999**, *103*, 6061. See also Loughnane, B. J.; Farrer, R. A.; Scodinu, A.; Fourkas, J. T. *J. Chem. Phys.* **1999**, *111*, 5116.

(21) Nikiel, L.; Hopkins, B.; Zerda, T. W. *J. Phys. Chem.* **1990**, *94*, 7458.

(22) Yi, J.; Jonas, J. *J. Phys. Chem.* **19961**, *100*, 16789.

(23) Crupi, V.; Maisano, G.; Majolino, D.; Migliardo, P.; Venuti, V. *J. Chem. Phys.* **1998**, *109*, 7394.

(24) Crupi, V.; Majolino, D.; Migliardo, P.; Venuti, V. *Nuovo Cimento* **1998**, *20D*, 2163.

(25) Crupi, V.; Magazù, S.; Majolino, D.; Maisano, G.; Migliardo, P. *J. Mol. Liq.* **1999**, *80*, 133.

(26) Zanotti, J. M.; Bellissent-Funel, M. C.; Chen, S. H. *Phys. Rev. E* **1999**, *59*, 3084 and references therein.

(27) Crupi, V.; Majolino, D.; Migliardo, P.; Venuti, V.; Magazù, S. *Steam, Water, and Hydrothermal Systems: Physics and Chemistry Meeting the Needs of Industry*; Tremaine, P. R., Hill, P. G., Irish, D. E., Balakrishnam, P. V., Eds.; NRC Press: Ottawa, 2000.

(28) Gorbatschow, W.; Arndt, M.; Stannarius, R.; Kremer, F. *Europhys. Lett.* **1996**, *35*, 719.

(29) Crupi, V.; Magazù, S.; Maisano, G.; Majolino, D.; Migliardo, P.; Venuto, S. *Phys. Chem. Liq.* **1994**, *26*, 263.

(30) Alvarez, F.; Alegria, A.; Colmenero, J. *Phys. Rev. B* **1991**, *44*, 7306 and references therein.

(31) Egelstaff, P. A. *J. Chem. Phys.* **1970**, *53*, 2590.

(32) Maisano, G.; Migliardo, P.; Fontana, M. P.; Bellissent-Funel, M. C.; Dianoux, A. J. *J. Phys. C: Solid State Phys.* **1985**, *18*, 1115 and references therein.

(33) Clark, R. J. H. *Advances in Infrared and Raman Spectroscopy*; Clark, R. J. H., Hester, R. E., Eds.; Heyden: London, 1978; p 109.

(34) Berne, B. J.; Pecora, R. *Dynamic Light Scattering;* Wiley: New York, 1976.

(35) Wang, C. H.; Wright, R. B. *Chem. Phys. Lett.* **1971**, *11*, 277.

(36) Graener, H.; Je, T. Q.; Laubereau, A. *J. Chem. Phys.* **1989**, *91*, 3413 and references therein.

(37) Janoschek, R. *The Hydrogen Bond I*; Shuster, P., Zundel, G., Sandorfy, C., Eds.; Amsterdam: North-Holland, 1976; p 166.

(38) Perez, J.; Zanotti, J.; Durand, D. *Biophys. J.* **1999**, *77*, 454.

(39) Magazù, S.; Maisano, G.; Majolino, D.; Migliardo, P. *Physical Chemistry of Aqueous Systems*; White, H. J., Sengers, J., Neumann, D., Bellows, J., Eds.; Wallingford: New York, 1995; p 361.

(40) Green, J.; Lacey, A.; Scheats, M. *J. Phys. Chem.* **1986**, *90*, 3958.

(41) Aliotta, F.; Vasi, C.; Maisano, G.; Majolino, D.; Mallamace, F.; Migliardo, P. *J. Chem. Phys.* **1986**, *84*, 4731.

(42) Sastriy, S.; Stanley, H.; Sciortino, F. *J. Chem. Phys.* **1994**, *100*, 5361.

(43) Volino, F.; Dianoux, A. J.; *Mol. Phys.* **1980**, *41*, 271.

(44) Crupi, V.; Magazù, S.; Majolino, D.; Migliardo, P.; Venuti, V.; Bellissent-Funel, M. C. *J. Phys. IV* **2000.** In press.

(45) Mel'nichenko, Y. B. *Hydrogen Bond Networks*; Bellissent-Funel, M. C., Dore, J. C., Eds.; Kluwer Academic Publisher: London, 1994; p 433.

(46) Pimentel, G. C.; McClellan, A. L. *The Hydrogen Bond II*; Shuster, P., Zundel, G., Sandorfy, C., Eds.; North-Holland: Amsterdam, 1976.